GeoHealth

RESEARCH ARTICLE
10.1029/2019GH000212

Key Points:
- The percentage of people who died in wind-related accidents is about double the deaths in accidents coded for weather other than wind
- The probability of wind-related accidents increased in low visibilities indicating that dust contributed to these incidents
- Ground visibility and dust optical depth were negatively correlated which highlights the increased risk of accidents in a dusty future

Supporting Information:
- Supporting Information S1

Correspondence to:
A. Bhattachan,
abhattachan@ucla.edu

Citation:
Bhattachan, A., Okin, G. S., Zhang, J., Vimal, S., & Lettenmaier, D. P. (2019). Characterizing the Role of Wind and Dust in Traffic Accidents in California. *GeoHealth*, *3*, 328–336. https://doi.org/10.1029/2019GH000212

Received 1 JUL 2019
Accepted 12 SEP 2019
Accepted article online 17 SEP 2019
Published online 28 OCT 2019

Author Contributions:
Conceptualization: Gregory S. Okin
Funding acquisition: Gregory S. Okin, Dennis P. Lettenmaier
Methodology: Gregory S. Okin
Project administration: Gregory S. Okin, Dennis P. Lettenmaier
Resources: Junzhe Zhang, Solomon Vimal
Software: Junzhe Zhang, Solomon Vimal
Supervision: Gregory S. Okin
Writing – review & editing: Gregory S. Okin, Dennis P. Lettenmaier

Characterizing the Role of Wind and Dust in Traffic Accidents in California

Abinash Bhattachan[1], **Gregory S. Okin**[1], **Junzhe Zhang**[1], **Solomon Vimal**[1], and **Dennis P. Lettenmaier**[1]

[1]Department of Geography, University of California, Los Angeles, CA, USA

Abstract Wind is a common ground transportation hazard. In arid regions, wind-blown dust is an added risk. Here, we analyzed the relationship between accidents and wind speed, dust events to study how they may have contributed to vehicular accidents in California. The California Highway Patrol reports information about weather conditions that potentially contributed to traffic accidents, including a code for wind but not for reduced visibility due to dust. For the three counties that contain the major dust source regions in California (the Mojave Desert and the Imperial Valley), we found greater daily maximum wind speed for days with accidents coded for wind compared to all days with accidents. The percentage of people injured in accidents attributed for weather other than wind and coded for wind were the same; however, the percentage of people who died in wind-related accidents was about double the deaths in accidents caused by weather other than wind. At ground meteorological stations closest to accidents, we found lower median minimum visibility for days with wind-related accidents compared to all days with accidents. Across the region, wind speed recorded at ground meteorological stations increased the probability of high satellite-derived dust optical depth values. Over the period of 2006 to 2016, the correlation between daily minimum visibility and daily maximum satellite-estimated dust optical depth was negative. Our analysis of the correlation between dust and accidents shows that with increased wind storm and dust-event frequency in the future, the risk of traffic incidents due to wind and dust could increase.

Plain Language Summary Wind-blown dust reduces visibility that can then lead to increased risk of accidents. While the California Highway Patrol reports information about adverse weather conditions that potentially contribute to traffic accidents like wind, it does not provide information for reduced visibility due to dust. To better understand the relationship between traffic incidents and hazardous weather condition caused by wind and/or dust, we use dust-related variables such as wind speed, visibility, and satellite-derived proxy for regional dust activity to determine the extent to which accidents between 2006 and 2016 that were reportedly caused by wind were also coincident with dust. Our work is important because the percentage of people who died in wind-related accidents was about double the deaths in accidents related to weather other than wind. We found that for all wind-related accidents as wind speed increased, visibility from weather stations closest to the accident location decreased. Furthermore, the likelihood of a wind-related accident increased in low visibilities. Our analysis also found a negative relationship between ground visibility and regional dust activity, which increases the future risk of vehicular accidents in a drier and dustier California.

1. Introduction

Atmospheric dust has important effects on Earth's hydrological, biogeochemical, and climate cycles (Goudie & Middleton, 2006; Okin et al., 2011; Ravi et al., 2011). Dust also carries allergens, spores, and microorganisms with negative effects to human health (see Crooks et al., 2016; Goudie, 2014; Middleton, 2017). Wind-blown dust can impair visibility for drivers, which can then lead to increased accident risks (Ashley et al., 2015; Goudie, 2014; Okin et al., 2011). While studies of the large-scale effects of dust in the Western United States often focus on wind erosion of surface soil and long-range transport of dust and its effects on Earth processes (e.g., Neff et al., 2008; Painter et al., 2010), there are few studies that focus on dust emitted from local dust sources that could create hazardous travel conditions (e.g., Baddock et al., 2013; Li et al., 2017). Dust-caused traffic accidents can be large and deadly. For example, a dust storm in California's San Joaquin Valley in late November 1991 resulted in near zero visibility, which led to 164 vehicular accidents in 33 collisions with 151 injuries and 17 deaths (Pauley et al., 1996). Laity (2003) reported that localized dust activity in the Lower Mojave Valley in California had led to fatal highway accidents. Although additional anecdotal reports of the wind- and dust-caused accidents are common in the popular press, there is relatively little work on the relationship between wind-blown dust and road accidents in the scientific literature (Ashley et al., 2015; Call et al., 2018; Goudie, 2014; Li et al., 2017; Pauley et al., 1996). Much of what literature does exist consists of case studies (e.g., Call et al., 2018; Pauley et al., 1996) or examines the distribution and prevalence of accidents reported to be due to wind or dust (e.g., Laity, 2003; Ashley et al., 2015; Goudie, 2014; Crooks et al., 2016; Li et al., 2017). Scientific studies of measured dust-generating meteorological conditions associated with motor vehicle accidents remain scarce. This is due, at least in part, to the fact that many wind- and dust-related accidents occur in remote areas where measurement stations are widely spread.

Dust can come from both natural sources such as disturbed alluvial fans, dry lakes, and floodplains (Ginoux et al., 2012) and anthropogenic sources such as agricultural fields and rangelands (Deetz et al., 2016; Pauley et al., 1996). In California, outside the now-controlled Owens River, the major sources of dust are the Mojave Desert and the Imperial Valley (including the area around the Salton Sea; Prospero et al., 2002; Goudie & Middleton, 2006; Ginoux et al., 2012). These two major California dust source areas are similar to many other contemporary sources of dust on Earth: topographic depressions in arid regions (Ginoux et al., 2012; Prospero et al., 2002). Satellite estimates derived from the Moderate Resolution Imaging Spectroradiometer (MODIS) instruments indicate that the highest concentrations of dust over the Mojave Desert and the Imperial Valley are observed between March and May, and on average, dust is detected between 7 and 28 days per year (Ginoux et al., 2012). Dust in this region is driven by synoptic scale meteorological patterns in spring that transport dust (Rivera Rivera et al., 2009; Hahnenberger & Nicoll, 2012); ground-based measurements of dust across the region are also consistent with satellite estimates (e.g., Hand et al., 2017).

In this study, we subset the record of accidents from the California Highway Patrol (CHP) from 2006 to 2016 to determine the extent to which accidents reported as wind related were also coincident with dust-related variables such as wind speed, visibility, and satellite-derived dust optical depth (DOD). DOD derived from optical spaceborne instruments is currently a coarse descriptor of atmospheric dust over the continents but has the potential, at least retrospectively, to link accident-causing dust events with regional conditions that promote dust production. The goal of this study is to elucidate the meteorological conditions that are associated with increased risk of wind- or dust-related accidents in Southern California.

2. Methods

2.1. Accident Data

Accident data were downloaded from the CHP's Statewide Integrated Traffic Record System for years 2006–2016 (http://iswitrs.chp.ca.gov/Reports/jsp/CollisionReports.jsp; access date: 9/27/2017). The data include the location (i.e., county, primary, and secondary roads) and date of each accident reported by the CHP during the period of interest. The data also include flags for weather conditions such as rain, fog, wind, and snow at the time when the accident occurred. Here, we were interested mostly in accidents that were caused by wind (code used: "G") in mostly rural or exurban areas that might be related to dust. To this end, we subset the data by selecting accidents in three desert counties (San Bernardino, Riverside, and Imperial) in Southern California that contain the majority of the Mojave, Colorado, and Sonoran Desert portions of California and which also account for about 13% of the total accidents in the state during this time period. We then extracted the accidents with the G flag from those three counties. Using the primary and secondary roads and county information from the accident data set, we used a geolocation method on Google Maps to retrieve the approximate latitude and longitude of each accident. We developed a Python program to automate behavior of a local browser session, which then generated latitude and longitude based on information in the accident data set: nearest intersection and county. The resulting approximate accident location is the location of the reported intersection in the accident data set.

2.2. Meteorological Data

We used subdaily wind speed and visibility data for 2006–2016 from the network of Automated Surface Observing Stations (ASOS) in California (https://mesonet.agron.iastate.edu/sites/networks.php?network=CA_ASOS; access date: 2/10/2018). Each accident was classified according to which ASOS station it was closest to (Euclidean distance in latitude-longitude space), and we extracted the daily maximum wind speed

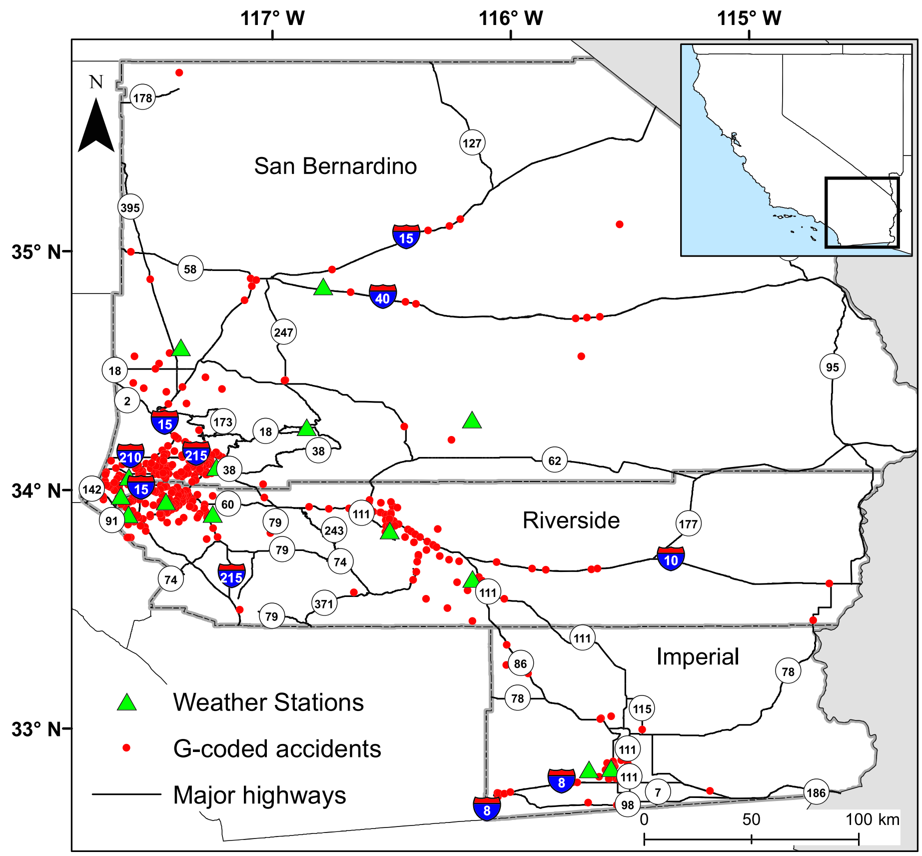

Figure 1. Wind-related (G-coded) accidents in Southern California along with the major highways, and weather stations in the region.

(WS_{max}) and minimum visibility ($VSBY_{min}$) for closest ASOS station for each day with an accident. Accidents with G codes were subset from this overall data set.

2.3. MODIS Deep Blue Aerosol Product

We used the daily MODIS collection 6 Deep Blue Level 2 (M-DB2) aerosol products for years 2006–2016 (Hsu et al., 2004). This product has near-daily high-resolution (~$0.1° \times 0.1°$) aerosol optical depth (AOD) estimates at multiple wavelengths (Ginoux et al., 2012; Hsu et al., 2004). Validation of AOD values with collocated ground-based measurements of AOD from the AERONET sites has been performed by Ginoux et al. (2012), who found that MODIS-derived products are well correlated (Pearson's $r = 0.85$) with ground measurements. We gridded the daily aerosol optical depth best estimate at 550 nm onto a regular 0.1° latitude-longitude grid using the nearest neighbor resampling method and cropped the pixels for the entire state of California. We chose the aerosol optical depth best estimate product at 550 nm wavelength because the quality control for cloud cover is already applied (Hsu et al., 2013). From these data, we generated daily rasters of DOD for California using the conditions suggested by Ginoux et al. (2012) to estimate DOD, that is, using an Angstrom exponent (α) threshold of 0.5 and single-scattering albedo (ω) criteria to filter out those pixels with sea salt and sulfate aerosols. Using the coordinates of ASOS weather stations, we extracted DOD values from a nine-pixel window containing the weather stations (i.e., 3×3 pixels with the center pixel being nearest-neighbor to the weather station coordinates). Subsequent analysis used the maximum value of DOD among the nine pixels, which is denoted as DOD_{max}.

2.4. Analytical Approach

We calculated the conditional probability of hourly wind speed above 6 m/s for visibility across all 14 weather stations for the entire weather record (Figure 1 and Table S1 of the supporting information). We chose 6 m/s as the critical threshold wind velocity as it conforms to a wind speed needed to initiate wind

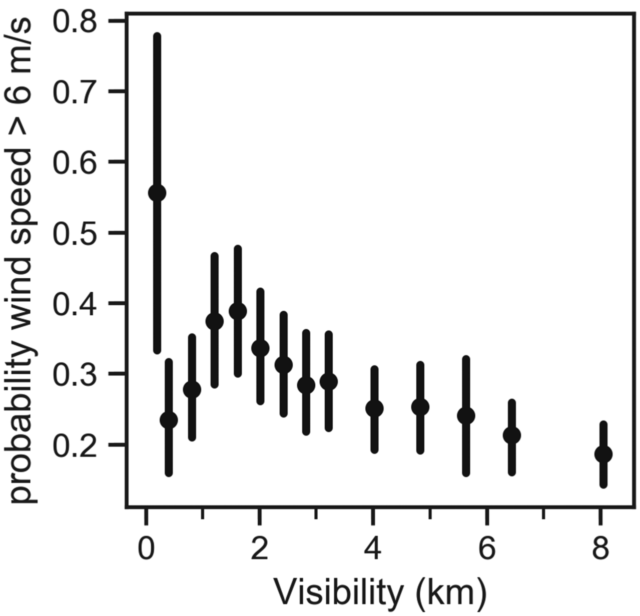

Figure 2. Probability that wind speed will be greater than the critical threshold velocity (6 m/s) for given visibility (km). The error bars represent ±1 standard error.

erosion and emit dust from the surface (Bagnold, 1941; Fryberger & Dean, 1979). We used the Spearman correlation coefficient, weighted by the inverse of the standard error, to determine the relationship between conditional probability of wind speed above 6 m/s and visibility (Emad & Bailey, 2017).

"Accident-days" were defined as days with accidents. We extracted median of WS_{max} and $VSBY_{min}$ from the 14 weather stations to represent the regional weather conditions on accident-days. For each G-coded accident, we used WS_{max} and $VSBY_{min}$ from the closest meteorological station. The median DOD_{max} at each station was also calculated for all accident-days. From these data, cumulative frequency distributions of median WS_{max}, median $VSBY_{min}$, and median DOD_{max} for accident-days were constructed. In addition, cumulative frequency distributions were constructed of WS_{max}, $VSBY_{min}$, and DOD_{max} on days with accidents with the G flag from individual stations closest to the G-coded accidents. We used a two-sample Kolmogorov-Smirnov (KS) test to determine if the distribution of WS_{max}, $VSBY_{min}$, and DOD_{max} of not G-coded accident-days differed from the distributions of G-coded accident-days. In addition, we calculated the conditional probability of days with DOD_{max} greater than 0.2 for a range of values of WS_{max} and $VSBY_{min}$ for both, not G-coded accident-days and G-coded accident-days. We used the Spearman correlation coefficient, weighted by the inverse of the standard error, to determine the relationship between conditional probability of DOD_{max} greater than 0.2 and WS_{max} and $VSBY_{min}$. We chose 0.2 as the minimum DOD_{max} to distinguish dust from background aerosols as in Ginoux et al. (2012).

3. Results

The total number of accidents in San Bernardino, Riverside, and Imperial counties were 283,964, 246,262, and 13,245, respectively, of which 328 (0.12%) in San Bernardino, 316 (0.13%) in Riverside, and 64 (0.50%) in Imperial were wind related (i.e., had a G weather code). The total number of accidents that were weather related (i.e., a weather code was provided by the CHP and did not take place on a clear day) was 68,575 (13%), in which 35,354 people were injured and 664 died; 368 people were injured and 17 died during wind-related accidents. Although the percentage of injured people in accidents caused by weather other than wind and by wind are the same (both 52%), the percentage of people who died in wind-related accidents is about double the deaths in accidents that were caused by weather other than wind (2.40% vs. 0.94%).

The data indicate that 29% of the wind-related accidents (204 out of 708) took place during the dust season (March–May; Ginoux et al., 2012) in the region. The probability of $WS_{max} \geq 6$ m/s generally decreases as $VSBY_{min}$ increases (weighted Spearman correlation coefficient, $\rho = -0.70$; $p < 0.01$; Figure 2). The relationship between WS_{max} and $VSBY_{min}$ for G-coded accident-days ($Accidents_{wind}$) is significant and negative ($\rho = -0.193$; $p < 0.01$, $WS_{max} = -0.33VSBY_{min} + 12.515$; blue line in Figure 3a), whereas for all other accident-days ($Accidents_{all}$), there is a weak positive and significant relationship ($\rho = 0.093$; $p < 0.01$, $WS_{max} = 0.056VSBY_{min} + 5.7451$; blue line in Figure 3b). Correspondingly, the joint distribution of WS_{max} and $VSBY_{min}$ shows considerable differences between $Accidents_{wind}$ and $Accidents_{all}$. G-coded accident-days occur more frequently on days with $WS_{max} \geq 6$ m/s, with the majority (58%) of G-coded accidents occur when $WS_{max} \geq 6$ m/s and $VSBY_{min} \leq 5$ km. For all accident-days ($Accidents_{all}$), WS_{max} rarely exceeds 8 m/s, and there are no accident-days with $WS_{max} \geq 15$ m/s.

There are significant differences between the distributions of WS_{max} from stations closest to a G-coded accident and median WS_{max} for all stations for accident-days (Figure 4a; KS test p value <0.01). The median WS_{max} at all stations for $Accidents_{all}$ was lower than that for the station closest for $Accidents_{wind}$ (6.0 vs. 9.7 m/s; Figure 4a). Similarly, there are statistically significant differences between the distributions of $VSBY_{min}$ of stations closest to a G-coded accident and median $VSBY_{min}$ for all stations for all accident-

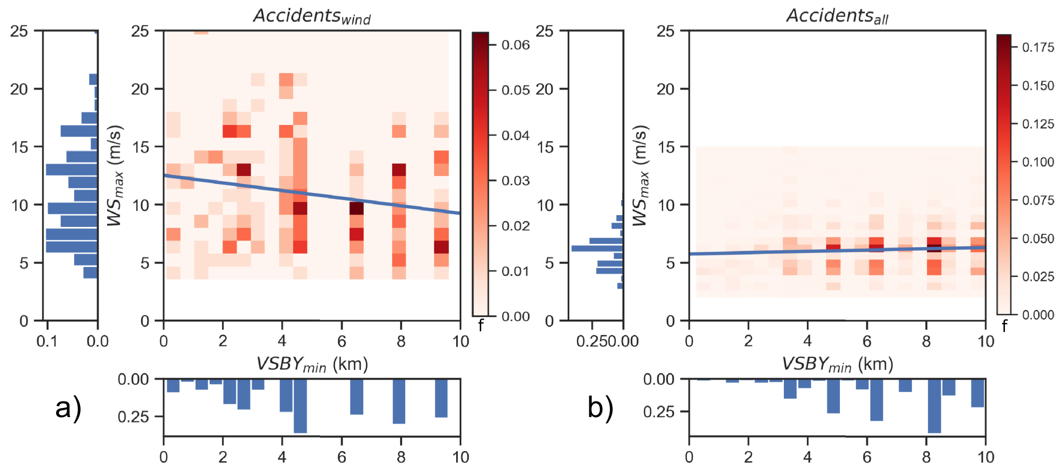

Figure 3. Joint probability distributions indicating the proportion of accidents: (a) all wind-related accidents (Accidents$_{wind}$); (b) all accidents (Accidents$_{all}$) occurring under combined conditions of WS$_{max}$ and VSBY$_{min}$.

days (Figure 4b; KS test p value <0.01). The median VSBY$_{min}$ at not G-coded station for all accident-days was greater than that for days and stations with G-coded accident (6.4 vs. 4 km; Figure 4b); 131 not G-coded accident-days (~40%) had median VSBY$_{min}$ < 5 km, whereas 149 (~62%) G-coded accidents at the closest station had VSBY$_{min}$ < 5 km. The differences are even starker when lower visibilities, in which dust is more likely to be present, are considered. Six not G-coded accident-days (~2%) had median VSBY$_{min}$ < 2 km, whereas nearly 28 (~11%) G-coded accidents at the closest station had VSBY$_{min}$ < 2 km.

There is some evidence that M-DB2-derived DOD observations capture atmospheric conditions that indicate surface conditions that contribute to G-coded accidents (Figure 4c); 95% of the G-coded accidents occurred when DOD$_{max}$ = 0 (no dust detected in the atmosphere by the satellite), whereas 99% of all other accident-days happened when DOD$_{max}$ = 0. However, the KS two sample test indicates that the two distributions are not statistically distinguishable (KS p value = 0.51; Figure 4c). We did not observe an increase in median WS$_{max}$ for all accident-days when DOD was equal to 0 compared to days when DOD$_{max}$ > 0 (median of WS$_{max}$ = 6 m/s in both cases). However, on G-coded accident-days, the median WS$_{max}$ was 10.2 m/s when DOD$_{max}$ = 0 and 11.7 m/s when DOD$_{max}$ > 0. Similarly, on G-coded accident-days, median VSBY$_{min}$ was lower when DOD$_{max}$ > 0 (median VSBY$_{min}$ = 4.8 km when DOD$_{max}$ = 0 and 2.6 km when DOD$_{max}$ > 0); 36 out of 708 (5%) of G-coded accident-days occurred when DOD$_{max}$ > 0, and among them, 18 accidents occurred when DOD$_{max}$ > 0.2.

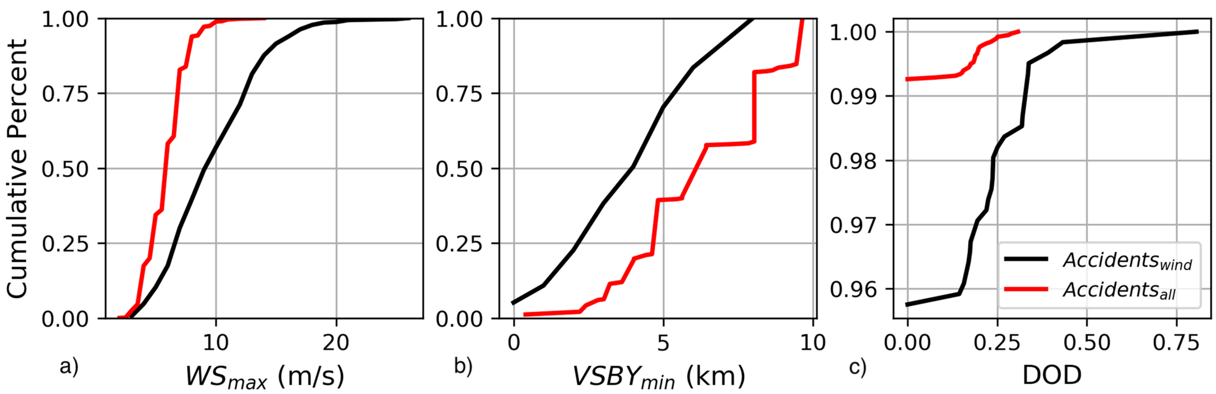

Figure 4. Cumulative percent of all accidents (Accidents$_{all}$) and wind-related accidents (Accidents$_{wind}$) for (a) WS$_{max}$, (b) VSBY$_{min}$, and (c) DOD$_{max}$. Note that the y-axis is different for Figure 4c.

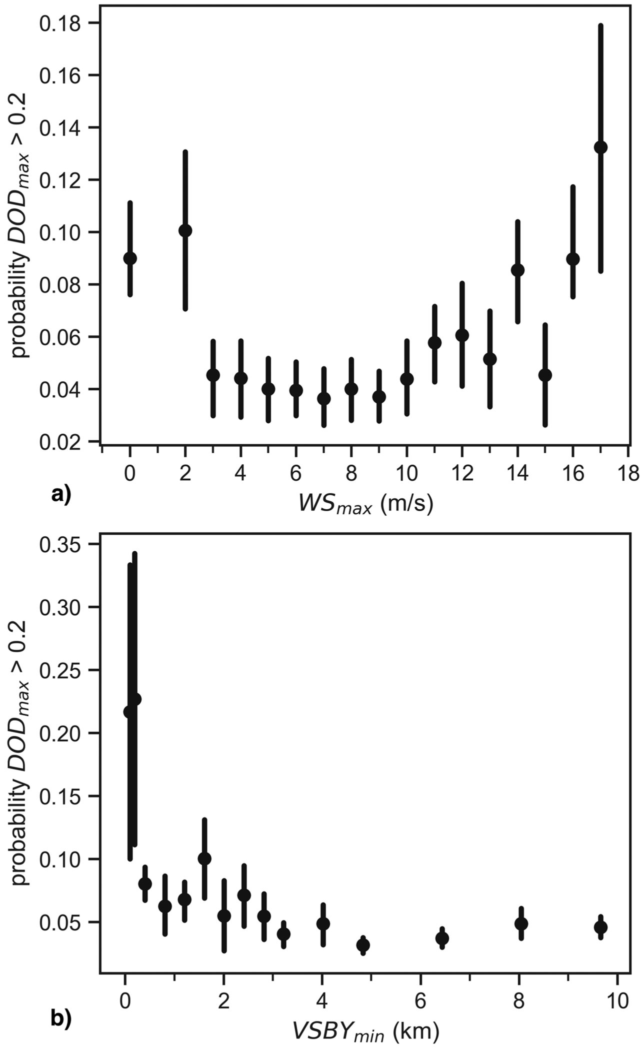

Figure 5. Probability that DOD_{max} is greater than a minimum threshold (0.2) for (a) WS_{max} and (b) $VSBY_{min}$.

Our results indicate that, as median $VSBY_{min}$ decreases, the probability of days with $DOD_{max} > 0.2$ increases (Figure 5b). There is a significant positive relationship between WS_{max} and the probability that $DOD_{max} > 0.2$ (weighted Spearman correlation coefficient, $\rho = 0.82$; $p < 0.01$; Figure 5a). The average probability of $DOD_{max} > 0.2$ when WS_{max} is 6 m/s is 0.04, but this increases to 0.061 when WS_{max} is greater than 6 m/s. For $WS_{max} > 9.7$ m/s (the median WS_{max} for G-coded accident-days from Figure 4a), the probability of $DOD_{max} > 0.2$ is 0.09. Similarly, the average probability of DOD > 0.2 when $VSBY_{min}$ is 5 km is 0.032, but increases to 0.093 when $VSBY_{min} < 5$ km (Figure 5b). The correlation between DOD > 0.2 and $VSBY_{min}$ is negative and significant (weighted Spearman correlation coefficient, $\rho = -0.68$; $p < 0.01$; Figure 5b).

4. Discussion

Adverse weather conditions such as rain, snow, fog, smoke, and dust can obscure a driver's vision and increase accident risk, and most weather-related accidents in the continental United States are not associated with wind or dust (Ashley et al., 2015). However, dust storms in our study region have led to hazardous travel conditions, which have resulted in fatalities (e.g., Laity, 2003), and our results show that in California, the percentage of deaths in wind-related accidents was more than twice than in all other weather-related accidents. Accidents that are reportedly caused by wind (G-coded) could be caused by high wind (blowing vehicles off the road or into other vehicles, or tipping vehicles over) or low visibility due to wind-generated dust. These meteorological variables are somewhat related, although not perfectly (Figure 2). This may reflect several factors such as spatiotemporal variability in dust emissivity of the surface, or the direction of the wind (i.e., dust may have affected road conditions but not been observed at the stations used here). Our meteorological and satellite-derived DOD data are not from the immediate locations of the accidents, so we acknowledge a mismatch between the conditions that might have caused an accident and what was recorded at the nearest station. The fact that there are nonetheless important relationships argues for the utility of this analysis.

Our results show that the incidence of G-coded accidents increases at high wind and low visibility conditions (Figures 3 and 4). Our results also show that 62% of the G-coded accidents occur on days where visibility measured at the nearest station is less than 5 km compared to 40% of the not G-coded accident-days. Maximum daily wind speed (WS_{max}) measured at the nearest station clearly has an impact on the likelihood of a G-coded accident, compared to accidents not related to wind (Figures 3 and 4). There are strong differences between G-coded accidents and not G-coded accidents in terms of visibility, particularly at low visibilities. When $VSBY_{min} < 5$ km, the likelihood of an accident being labeled as "wind related" increases from 0.34 to 0.70 (106% increase). When $WS_{max} > 6$ m/s, the increased likelihood of a G-coded accident increases from 0.40 to 0.83 (107% increase). When considering joint distribution of $WS_{max} > 6$ m/s and $VSBY_{min} < 5$ km, the increased likelihood of an accident labeled as wind related increases from 0.11 to 0.58 (~420% increase). When DOD > 0.2, the probability of a G-coded accident increases from 0.003 to 0.03 (900% increase). This suggests that the CHP-applied wind label (G) is picking up times when the accident is, in fact, caused by reduced visibility due to blowing dust. Thus, there is evidence that the measured variables such as WS_{max}, $VSBY_{min}$, and even DOD_{max} predict likelihoods of increased wind-related accidents and that some of these are related to wind only whereas others are related to windborne dust.

Visibility is commonly used as proxy for dust activity (e.g., Baddock et al., 2014; Chung et al., 2003; Engelstaedter et al., 2003; Goudie & Middleton, 1992). Our results show that the median daily $VSBY_{min}$ and median daily DOD_{max} are negatively correlated; when the probability of DOD > 0.2 increases, visibility on the ground is lower (Figure 5b). We take this as an indication that DOD_{max} might be useful as an index of dust at the surface in this region, similar to visibility in other regions (e.g., Baddock et al., 2014; Chung et al., 2003). With regard to traffic hazards, this result is significant; our results show that in the last decade, 36 accidents out of 708 G-coded accidents happened on days with $DOD_{max} > 0$ in the three counties near two major sources of dust in California. Observed patterns or changes in DOD_{max} could be used by officials to take measures in certain stretches of highway during certain times to alert drivers to the hazard of a dust storm in a form of weather advisory and what to do in case one happens.

Nonetheless, although visibility at the surface (a proxy for dust activity) and the conditional probability that DOD > 0.2 are significantly negatively correlated, it is important to realize that they measure fundamentally different things. This is perhaps a limitation owing to the temporal mismatch between the data sets that we used. Visibility is a proxy for dust concentration at the surface, whereas DOD is measuring light attenuation in a column through the atmosphere daily at a specific time (Hsu et al., 2004, 2013). Although DOD derived from M-DB2 is available on a daily basis, it is however not a daily representation of regional dust activity. Dust storms that occur close to the ground might be sudden and short-lived and might not be reflected in the M-DB2 data set. In other words, we caution that DOD does not measure what a driver experiences, and it is almost certain that these analyses are missing some events when DOD would have been greater than 0.2. In fact, the number of days during the dust season with DOD > 0.2 for areas near the Mojave Desert and the Salton Sea is much smaller in our analysis as compared to Ginoux et al. (2012). Nonetheless, there is a significant relationship that is apparent mostly at very low visibilities. This correlation (weighted $\rho = -0.86$, $p < 0.01$; Figure 5b) is comparable to correlations between visibility and other measures (including AERONET) that have been published (Mahowald et al., 2007).

Despite the hazardous nature of episodic wind and dust storms, the effect of dust storms on traffic incidents is highly dependent on the timing of the storm. For example, one of the worst traffic incidents recorded in the San Joaquin Valley (Pauley et al., 1996) took place during an afternoon of a major U.S. holiday weekend. The early warning system for dust storms issued by the National Weather Service encouraging people to avoid travel has been increasingly used in the region since 2007 (Ashley et al., 2015) and may also have contributed to reduced traffic incidents.

There is some evidence that the dust loading in the southwestern United States has been increasing in the past two decades (Brahney et al., 2013; Hand et al., 2016) and is expected to increase globally in the future (Tegen et al., 2004). Others have argued that the future might be less dusty (e.g., Mahowald & Luo, 2003). The U.S. Southwest (including California) is expected to also get drier in the coming decades (Cook et al., 2014; Seager et al., 2007; Seager & Vecchi, 2010), and a recent study showed that bare ground cover is strongly correlated with dust event frequency in California, which is expected to also increase in the coming decades (Pu & Ginoux, 2017). As climate and land-use change are tightly coupled with dust emissions (Okin & Reheis, 2002; Neff et al., 2008; Cook et al., 2009; Munson et al., 2011), increased aridity and land-use change in the region can increase surface erodibility and dust emissions by reducing the amount of available soil moisture and promoting vegetation die-off. As such, a future with increased probability of dust emissions in the region (Hand et al., 2016; Pu & Ginoux, 2017) could worsen regional air quality with serious consequences to human health, regional climate and hydrologic cycles, and vehicular transportation.

5. Conclusions

Dust storms disrupt travel and compromise highway safety by impairing visibility for drivers, which can then lead to increased accident risks. In California, several studies have documented the role of dust in traffic accidents. Our study focused on an analysis of dust-related variables such as wind speed, visibility, and satellite-derived DOD and their relationship with traffic accidents. Using the accident data set from the CHP that flagged wind-related accidents, we found that twice as many people died in wind-related accidents than other accidents caused by weather other than wind. We showed that the relationship between maximum wind speed and minimum visibility from stations closest to a wind-related accident is significant and negative, whereas for all other accidents, this relationship is positive. We also showed that the probability of wind-related accidents likely increased in low visibilities, indicating that dust could have contributed to these incidents. The probability of a wind-related accident increased with increasing wind speed and/or decreasing visibility. Although the satellite-derived DOD characterizes regional dust activity, we found that visibility and DOD were negatively correlated, which further highlights the increased risk of accidents in a dusty future.

Conflict of Interest

The authors declare no conflicts of interest relevant to this study.

Acknowledgments
We are grateful to the California Highway Patrol and the MODIS Deep Blue team at NASA (https://deepblue.gsfc.nasa.gov) for the data used in our work. Funding for this work was provided by the University of California Office of the President via Multicampus Research Programs and Initiatives (MRPI; Climate and Health Interdisciplinary Research Program). We thank two anonymous reviewers for their thoughtful and thorough comments. All data used in our work can be found online (https://figshare.com/s/c437f94611ef9286edae).

References

Ashley, W. S., Strader, S., Dziubla, D. C., & Haberlie, A. (2015). Driving blind: Weather-related vision hazards and fatal motor vehicle crashes. *Bulletin of the American Meteorological Society*, *96*(5), 755–778.

Baddock, M. C., Strong, C. L., Leys, J., Heidenreich, S., Tews, E., & McTainsh, G. H. (2014). A visibility and total suspended dust relationship. *Atmospheric Environment*, *89*, 329–336.

Baddock, M. C., Strong, C. L., Murray, P. S., & McTainsh, G. H. (2013). Aeolian dust as a transport hazard. *Atmospheric Environment*, *71*, 7–14.

Bagnold, R. (1941). *The physics of wind blown sand and desert dunes* (265 pp.). London, UK: Methuen.

Brahney, J., Ballantyne, A., Sievers, C., & Neff, J. (2013). Increasing Ca^{2+} deposition in the western US: The role of mineral aerosols. *Aeolian Research*, *10*, 77–87.

Call, D. A., Wilson, C. S., & Shourd, K. N. (2018). Hazardous weather conditions and multiple-vehicle chain-reaction crashes in the United States. *Meteorological Applications*, *25*(3), 466–471.

Chung, Y., Kim, H., Park, K., Jhun, J., & Chen, S. (2003). Atmospheric loadings, concentrations and visibility associated with sandstorms: Satellite and meteorological analysis. *Water, Air, & Soil Pollution: Focus*, *3*(2), 21–40.

Cook, B. I., Miller, R. L., & Seager, R. (2009). Amplification of the North American "Dust Bowl" drought through human-induced land degradation. *Proceedings of the National Academy of Sciences*, *106*(13), 4997–5001.

Cook, B. I., Smerdon, J. E., Seager, R., & Coats, S. (2014). Global warming and 21st century drying. *Climate Dynamics*, *43*(9-10), 2607–2627.

Crooks, J. L., Cascio, W. E., Percy, M. S., Reyes, J., Neas, L. M., & Hilborn, E. D. (2016). The association between dust storms and daily non-accidental mortality in the United States, 1993–2005. *Environmental Health Perspectives*, *124*(11), 1735.

Deetz, K., Klose, M., Kirchner, I., & Cubasch, U. (2016). Numerical simulation of a dust event in northeastern Germany with a new dust emission scheme in COSMO-ART. *Atmospheric Environment*, *126*, 87–97.

Emad, A., & Bailey, P. (2017). wCorr: Weighted correlations. R package version 1.9.1. https://CRAN.R-project.org/package=wCorr

Engelstaedter, S., Kohfeld, K., Tegen, I., & Harrison, S. (2003). Controls of dust emissions by vegetation and topographic depressions: An evaluation using dust storm frequency data. *Geophysical Research Letters*, *30*(6), 1294. https://doi.org/10.1029/2002GL016471

Fryberger, S. G., & Dean, G. (1979). Dune forms and wind regime. In E. D. McKee (Ed.), *a study of global sand seas* (Vol. 1052, pp. 137–169). U.S: Geol. Surv. Prof. Pap.

Ginoux, P., Prospero, J. M., Gill, T. E., Hsu, N. C., & Zhao, M. (2012). Global-scale attribution of anthropogenic and natural dust sources and their emission rates based on MODIS Deep Blue aerosol products. *Reviews of Geophysics*, *50*, RG3005. https://doi.org/10.1029/2012rg000388

Goudie, A., & Middleton, N. (2006). *Desert dust in the global system*. Berlin: Springer Verlag.

Goudie, A. S. (2014). Desert dust and human health disorders. *Environment International*, *63*, 101–113.

Goudie, A. S., & Middleton, N. J. (1992). The changing frequency of dust storms through time. *Climatic Change*, *20*(3), 197–225.

Hahnenberger, M., & Nicoll, K. (2012). Meteorological characteristics of dust storm events in the eastern Great Basin of Utah, USA. *Atmospheric Environment*, *60*, 601–612.

Hand, J., White, W., Gebhart, K., Hyslop, N., Gill, T., & Schichtel, B. (2016). Earlier onset of the spring fine dust season in the southwestern United States. *Geophysical Research Letters*, *43*, 4001–4009.

Hand, J. L., Gill, T. E., & Schichtel, B. A. (2017). Spatial and seasonal variability in fine mineral dust and coarse aerosol mass at remote sites across the United States. *Journal of Geophysical Research: Atmospheres*, *122*, 3080–3097. https://doi.org/10.1002/2016jd026290

Hsu, N. C., Jeong, M.-J., Bettenhausen, C., Sayer, A. M., Hansell, R., Seftor, C. S., et al. (2013). Enhanced Deep Blue aerosol retrieval algorithm: The second generation. *Journal of Geophysical Research: Atmospheres*, *118*, 9296–9315. https://doi.org/10.1002/jgrd.50712

Hsu, N. C., Tsay, S.-C., King, M. D., & Herman, J. R. (2004). Aerosol properties over bright-reflecting source regions. *IEEE Transactions on Geoscience and Remote Sensing*, *42*(3), 557–569.

Laity, J. (2003). Aeolian destabilization along the Mojave River, Mojave Desert, California: Linkages among fluvial, groundwater, and aeolian systems. *Physical Geography*, *24*(3), 196–221.

Li, J., Kandakji, T., Lee, J. A., Tatarko, J., Blackwell, J. III, Gill, T. E., & Collins, J. D. (2017). Blowing dust and highway safety in the southwestern United States: Characteristics of dust emission "hotspots" and management implications. *Science of the Total Environment*, *621*, 1023–1032.

Mahowald, N., Ballantine, J. A., Feddema, J., & Ramankutty, N. (2007). Global trends in visibility: Implications for dust sources. *Atmospheric Chemistry and Physics*, *7*, 3309–3339. https://doi.org/10.5194/acp-7-3309-2007

Mahowald, N. M., & Luo, C. (2003). A less dusty future? *Geophysical Research Letters*, *30*(17), 1903. https://doi.org/10.1029/2003GL017880

Middleton, N. (2017). Desert dust hazards: A global review. *Aeolian Research*, *24*, 53–63.

Munson, S. M., Belnap, J., & Okin, G. S. (2011). Responses of wind erosion to climate-induced vegetation changes on the Colorado Plateau. *Proceedings of the National Academy of Sciences*, *108*(10), 3854–3859. https://doi.org/10.1073/pnas.1014947108

Neff, J., Ballantyne, A., Farmer, G., Mahowald, N., Conroy, J., Landry, C., et al. (2008). Increasing eolian dust deposition in the western United States linked to human activity. *Nature Geoscience*, *1*(3), 189.

Okin, G. S., Bullard, J. E., Reynolds, R. L., Ballantine, J. A. C., Schepanski, K., Todd, M. C., et al. (2011). Dust: Small-scale processes with global consequences. *Eos, Transactions of the American Geophysical Union*, *92*(29), 241–242.

Okin, G. S., & Reheis, M. C. (2002). An ENSO predictor of dust emission in the southwestern United States. *Geophysical Research Letters*, *29*(9), 1332. https://doi.org/10.1029/2001GL014494

Painter, T. H., Deems, J. S., Belnap, J., Hamlet, A. F., Landry, C. C., & Udall, B. (2010). Response of Colorado River runoff to dust radiative forcing in snow. *Proceedings of the National Academy of Sciences*, *107*(40), 17,125–17,130. https://doi.org/10.1073/pnas.0913139107

10.1029/2019GH000212

Pauley, P. M., Baker, N. L., & Barker, E. H. (1996). An observational study of the "Interstate 5" dust storm case. *Bulletin of the American Meteorological Society*, *77*(4), 693–720.

Prospero, J. M., Ginoux, P., Torres, O., Nicholson, S. E., & Gill, T. E. (2002). Environmental characterization of global sources of atmospheric soil dust identified with the Nimbus 7 Total Ozone Mapping Spectrometer (TOMS) absorbing aerosol product. *Reviews of Geophysics*, *40*(1), 1002. https://doi.org/10.1029/2000RG000095

Pu, B., & Ginoux, P. (2017). Projection of American dustiness in the late 21st century due to climate change. *Scientific Reports*, *7*(1), 5553.

Ravi, S., D'Odorico, P., Breshears, D. D., Field, J. P., Goudie, A. S., Huxman, T. E., et al. (2011). Aeolian processes and the biosphere. *Reviews of Geophysics*, *49*, RG3001. https://doi.org/10.1029/2010RG000328

Rivera, N. I. R., Gill, T. E., Gebhart, K. A., Hand, J. L., Bleiweiss, M. P., & Fitzgerald, R. M. (2009). Wind modeling of Chihuahuan Desert dust outbreaks. *Atmospheric Environment*, *43*(2), 347–354.

Seager, R., Ting, M., Held, I., Kushnir, Y., Lu, J., Vecchi, G., et al. (2007). Model projections of an imminent transition to a more arid climate in southwestern North America. *Science*, *316*(5828), 1181–1184.

Seager, R., & Vecchi, G. A. (2010). Greenhouse warming and the 21st century hydroclimate of southwestern North America. *Proceedings of the National Academy of Sciences*, *107*(50), 21,277–21,282. https://doi.org/10.1073/pnas.0910856107

Tegen, I., Werner, M., Harrison, S., & Kohfeld, K. (2004). Relative importance of climate and land use in determining present and future global soil dust emission. *Geophysical Research Letters*, *31*, L05105. https://doi.org/10.1029/2002GL016471